Applied Ocean Research 86 (2019) 40–46

Contents lists available at ScienceDirect

Applied Ocean Research

journal homepage: www.elsevier.com/locate/apor

Path following control of fully-actuated autonomous underwater vehicle in presence of fast-varying disturbances

Habib Choukri Lamraoui*, Zhu Qidan

Automation College, Harbin Engineering University, China

ARTICLE INFO

Keywords:
Autonomous underwater vehicles
Active disturbances rejecter control
Generalized extended state observer
Harmonic extended state observer

ABSTRACT

This paper presents an improved active disturbances rejecter control (ADRC) for path following control of autonomous underwater vehicles under significant fast-varying disturbances caused by waves and sea currents. Two significant and efficient improvements are introduced to the traditional ADRC in order to accomplish this task. First, a generalized ESO (GESO) and Harmonic ESO (HESO) were designed to achieve a high disturbances estimation quality. Secondly, two AUV path following controllers based on ADRC-GESO and ADRC-HESO were designed to ensure a high performance tracking in presence of periodic-type disturbances. Finally, numerical simulations were performed and the obtained results showed very significant enhancements of robustness and tracking accuracy by the proposed methods compared to conventional ADRC.

1. Introduction

Autonomous Underwater Vehicles (AUVs) are mobile platforms that operate undersea independent of human intervention. Nowadays, AUVs have been widely studied and took part in many research works due to their large domain of applications in ocean exploration [1]; military domain (surveillance, reconnaissance, inspections, and mine countermeasures) [2], seafloor mapping, oil industry [3], fisheries [4], and geoscience research [5].

Considerable studies and researches have been devoted to the path following control of the AUVs, adaptive trajectory tracking control for fully-actuated autonomous underwater vehicles (AUVs) are proposed in [6], and robust and heuristic fuzzy logic control is adopted in [7] for AUV 3D path following under system uncertainties. The most important challenge in the control design for AUVs is to cope with uncertainties and disturbances effects. Therefore, more robust control approaches have been considered for this purpose; i.e., a continuous robust integral of the sign of the error (RISE) control structure is used for a coupled fully-actuated AUV in presence of disturbances and uncertainties in [8], an adaptive fuzzy reaching law controller (AFRLC) for tracking control of uncertain full-actuated underwater vehicles (FAUV) in the presence unknown external disturbances is presented in [9]; hierarchical image-based visual servoing (IBVS) strategy for dynamic positioning of a fully-actuated underwater vehicle in [10]; and a nonlinear adaptive controller for dynamic positioning problems of AUVs in [11].

One of the most promising approaches in disturbances rejection is the active disturbances rejecter control (ADRC) presented in the 1990s by Han [12]. This control technique showed very encouraging results in the robotic field, such as unmanned aerial vehicles (UAV) control [13], and mobile robots [14,15]. ADRC controllers have been considered for marine vehicles control in presence of uncertainties and disturbances; for the path following control of an Unmanned Surface Vessel (USV) in [16,17], and for the AUV control in [18,19]. Despite the remarkable effectiveness of the ADRC in the above studies, traditional ESO-based controllers are primarily focusing on dealing with constant or slow-varying disturbances, which provides an insufficient estimation and tracking performances in presence of fast-varying type disturbances, as illustrated in [20,21]. However, the disturbances induced by waves and wind are rarely constant as claimed in [10,11,16], but quite the contrary; the fast time-varying sinusoidal type is the common model used to govern the external disturbances in AUV control [22–26].

In this paper, we propose two approaches for the enhancement of the conventional ADRC-based path following control of fully-actuated AUVs in presence of fast time-varying sinusoidal-like disturbances. First, by increasing the order of the ESO in order to consider the dynamics of the time-varying disturbances. Secondly, by applying the harmonic ESO developed in [27]. According to the best of our knowledge, this is the first time to design a generalized or high-order ESO-based ADRC and HESO-based ADRC in path following control of AUVs. In this context, numerical simulations are performed and the obtained results are discussed. Then, the effectiveness of both of the improved ADRCs and the traditional ADRC in rejecting complex and fast varying

* Corresponding author.
E-mail addresses: habib_choukri@yahoo.com (H.C. Lamraoui), zhuqidan@hrbeu.edu.cn (Z. Qidan).

https://doi.org/10.1016/j.apor.2019.02.015
Received 13 November 2018; Received in revised form 14 February 2019; Accepted 20 February 2019
Available online 28 February 2019
0141-1187/

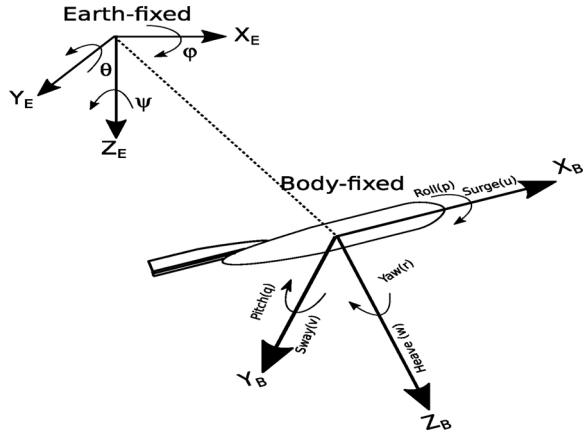

Fig. 1. coordinate system.

disturbances are compared, since the comparison between the ADRC and PID has been widely addressed in the literature.

The paper is structured as follows. Section 2 presents the AUV modelling. The design of the improved ADRCs based control law for the AUV to track the desired path is developed in Section 3. Numerical simulation results and discussion are provided in Section 4. Finally, conclusions are provided in Section 5.

2. System presentation

2.1. Kinematic model

The kinematic description represents the motion of the vehicle regardless of the effect of the forces acting on it. For this, the earth reference frame {E} and body-fixed reference frame {B} are employed as shown in Fig. 1.

The different degrees of freedom of the AUV are detailed in Table 1, and the position and velocity vectors of the AUV defined in the body frame {B} are χ and υ, respectively, as:

$$\chi = [x, y, z, \varphi, \theta, \psi] \tag{1}$$

$$\upsilon = [u, v, w, p, q, r] \tag{2}$$

The motion of the AUV is described by:

$$\dot{\eta} = R(\eta)^{*}\upsilon \tag{3}$$

where $\dot{\eta}$ is the velocity vector expressed in the earth frame {E}, and R is the transformation matrix between {B} and {E} determined by

$$R(\eta) = diag\{R1(\varphi, \theta, \psi), R2(\varphi, \theta, \psi)\} \tag{4}$$

with R_1 is a derivation of the rotation matrix and R_2 is a derivation of the coordinate transform matrix.

$$R1 = \begin{bmatrix} C\theta C\psi & -C\varphi S\psi + S\varphi S\theta C\psi & S\varphi S\psi + C\varphi S\theta C\psi \\ C\theta S\psi & C\varphi C\psi + S\varphi S\theta S\psi & -S\varphi C\psi + C\varphi S\theta S\psi \\ -S\theta & S\varphi C\theta & C\varphi C\theta \end{bmatrix} \tag{5}$$

$$R2 = \begin{bmatrix} 1 & S\varphi T\theta & C\varphi T\theta \\ 0 & C\varphi & -S\varphi \\ 0 & S\varphi/C\theta & C\varphi/C\theta \end{bmatrix} \tag{6}$$

where C. = cos(.), S. = sin(.), and T. = tan.

2.2. Dynamic model

In the dynamic study, the forces acting on the system and its physical characteristics are taken into consideration while studying the motion of the robot. Due to the complexity of these forces and the AUV's dynamics, the following assumptions have been made to simplify the AUV's model and the control design task as in [28]:

- The AUV operates at a low speed.
- The AUV is symmetric via the XZ and YZ planes.
- Pitch and roll movements are neglected.

After considering these previous assumptions, the simplified kinematics are represented by

$$\begin{bmatrix} \dot{x} \\ \dot{y} \\ \dot{\psi} \end{bmatrix} = \begin{bmatrix} C\psi & -S\psi & 0 \\ S\psi & C\psi & 0 \\ 0 & 0 & 1 \end{bmatrix} \begin{bmatrix} u \\ v \\ r \end{bmatrix} \tag{7}$$

The full AUV's 4 ° of freedom (DOF) dynamic model is

$$M\dot{\nu} + C(\nu)\nu + D(\nu)\nu + g(\eta) = \tau + \tau_{\omega} \tag{8}$$

where M is the mass and inertia matrix, C is the Coriolis and centripetal matrix, D is the hydrodynamic dumping matrix, and g is the gravitational and buoyancy matrix.

Eq. (8) is rewritten as:

$$\begin{cases} (m - X_{\dot{u}})\dot{u} - (X_u + X_{u|u|}\,|u|)u - (m - Y_{\dot{v}})vr = \tau_x + \tau_{w1} \\ (m - Y_{\dot{v}})\dot{v} - (Y_v + Y_{v|v|}\,|v|)v + (m - X_{\dot{u}})ur = \tau_y + \tau_{w2} \\ (m - Z_{\dot{\omega}})\dot{\omega} - (Z_{\omega} + Z_{\omega|\omega|}\,|\omega|)\omega = \tau_{\omega} + \tau_{w3} \\ (I_z - N_{\dot{r}})\dot{r} - (N_r + N_{r|r|}\,|r|)r + (X_{\dot{u}} + Y_{\dot{v}})uv = \tau_r + \tau_{w4} \end{cases} \tag{9}$$

By considering the assumptions made in the previous section and the full AUV's 4 DOF dynamic model, the one degree of freedom (surge) dynamic equation is:

$$m_{11}\dot{u} - d_{11}u - m_{22}vr = \tau_x + \tau_{w1} \tag{10}$$

where

$$\begin{cases} m_{11} = m - X_{\dot{u}} \\ m_{22} = m - Y_{\dot{v}} \\ d_{11} = X_u + X_{u|u|}\,|u| \end{cases} \tag{11}$$

With the variables are defined in Table 2.

Table 1
Degrees of freedom of the AUV.

Degree Of Freedom	Positions and Euler angles	Linear and angular velocities
motions in the x-direction (Surge)	x	u
motions in the y-direction (Sway)	y	v
motions in the z-direction (Heave)	z	ω
rotation about x-axis (Pitch)	φ	p
rotation about y-axis (Roll)	θ	q
rotation about z-axis (Yaw)	ψ	r

Table 2
variables definition.

`Variable	Definition
m	Masse
$X_{\dot{u}}$, $Y_{\dot{v}}$, $Z_{\dot{\omega}}$, $N_{\dot{r}}$	hydrodynamic added mass terms
X_u, Y_v, Z_ω, N_r	Linear hydrodynamic damping terms
$X_{u\|u\|}$, $Y_{v\|v\|}$, $Z_{\omega\|\omega\|}$, $N_{r\|r\|}$	quadratic hydrodynamic damping terms
τ_x, τ_y, τ_ω, τ_r	Control inputs
τ_{w1}, τ_{w2}, τ_{w3}, τ_{w4}	External disturbances induced forces

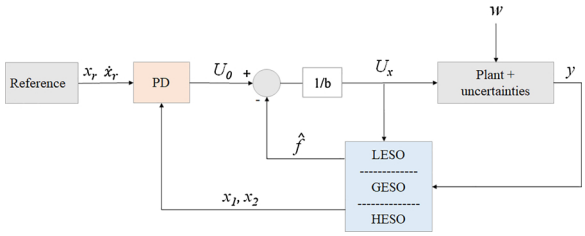

Fig. 2. ADRC general scheme for 1 DOF.

Table 3
AUV's parameters used in the simulation.

mass and inertia	Damping coefficients (Ns/m)
m_{11} = 215 [Kg]	d_{11} = 70 + 100 |u |
m_{22} = 265 [kg]	d_{22} = 100 + 200 |v |
m_{33} = 265 [Kg]	d_{33} = 100 + 200 |ω |
m_{44} = 80 [Kg.m^2]	d_{44} = 50 + 100 |r |

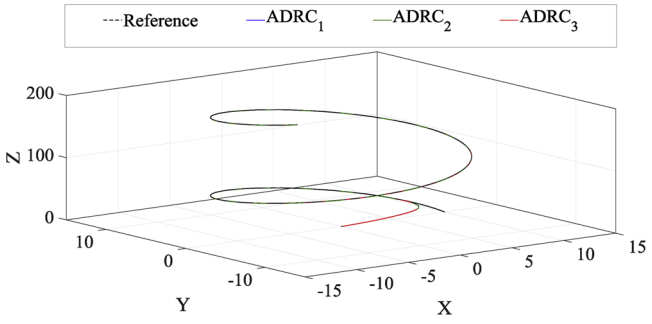

Fig. 3. 3-D path following.

3. Control design

3.1. GESO

According to [28], the 1DOF dynamic equation of the motion can be expressed as:

$$\dot{x} = 1/m_{11}(d_{11}\dot{x} + m_{22}\dot{y}\dot{\psi} + \tau_x) + \tau_{w1} \tag{12}$$

After introducing the disturbance function f_x into Eq. (12), the state space form of the system is written as

$$\begin{cases} \dot{x}_1 = x_2 \\ \dot{x}_2 = f_x(\dot{x}, \dot{y}, \dot{\psi}, t, \tau_{w1}) + b_x U_x \\ y = x_1 \end{cases} \tag{13}$$

The system will then be extended by two extras state variables (x_3, x_4, x_5) in place of the conventional one-state extension

$$\begin{cases} x_3 = f_x(\dot{x}, \dot{y}, \dot{\psi}, t, w) \\ x_4 = \dot{f}_x(\dot{x}, \dot{y}, \dot{\psi}, t, w) \\ x_5 = \ddot{f}_x(\dot{x}, \dot{y}, \dot{\psi}, t, w) \end{cases} \tag{14}$$

which estimates the total disturbances function and its first derivation, and the extended system state is presented below

$$\begin{cases} \dot{x}_1 = x_2 \\ \dot{x}_2 = x_3 + b_x U_x \\ \dot{x}_3 = \dot{f}_x = h = x_4 \\ \dot{x}_4 = \ddot{f}_x = \dot{h} = x_5 \end{cases} \tag{15}$$

The following fifth order LESO is then designed for the above system.

$$\begin{cases} \dot{z}_1 = z_2 - \beta_1 e_1 \\ \dot{z}_2 = z_3 - \beta_2 e_1 + b_x U_x \\ \dot{z}_3 = z_4 - \beta_3 e_1 \\ \dot{z}_4 = z_5 - \beta_4 e_1 \\ \dot{z}_5 = -\beta_5 e_1 \end{cases} \tag{16}$$

where z_i and β_i are the estimator's state variables and parameters, respectively.

To simplify the tuning of the parameters of the Linear ESO and the controller, they have been set as in Eq. (17), and the tuning is reduced from 7 to 2 parameters.

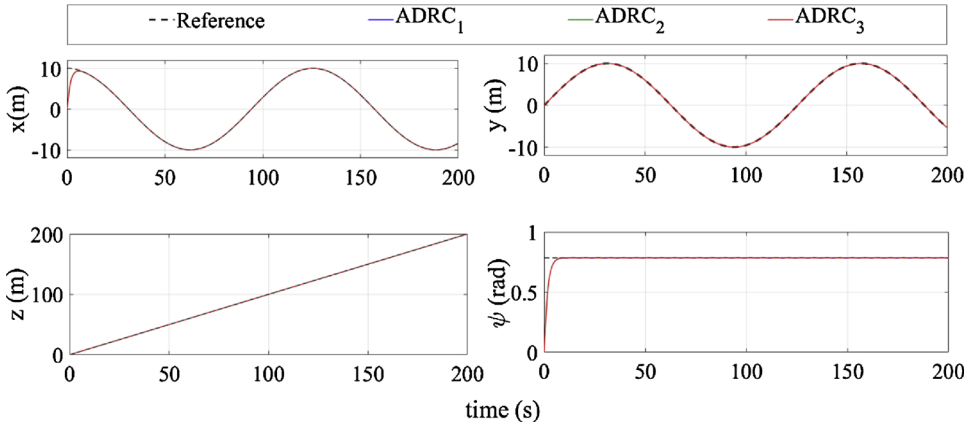

Fig. 4. Positions tracking.

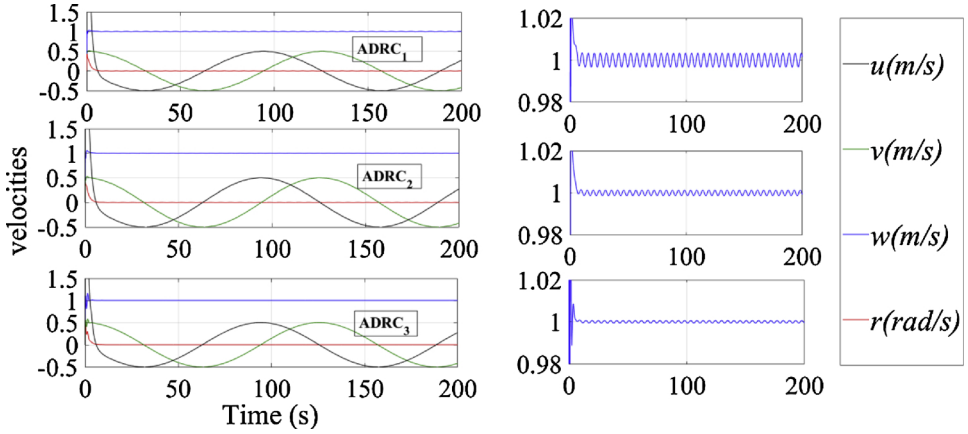

Fig. 5. Velocities.

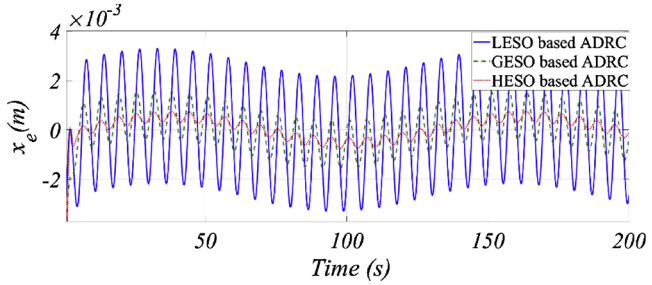

Fig. 6. Tracking errors comparison of HESO, GESO, and traditional LESO in surge tracking.

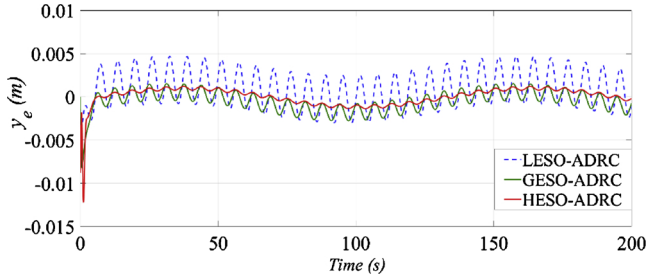

Fig. 7. Tracking errors comparison of HESO, GESO and traditional LESO in sway tracking.

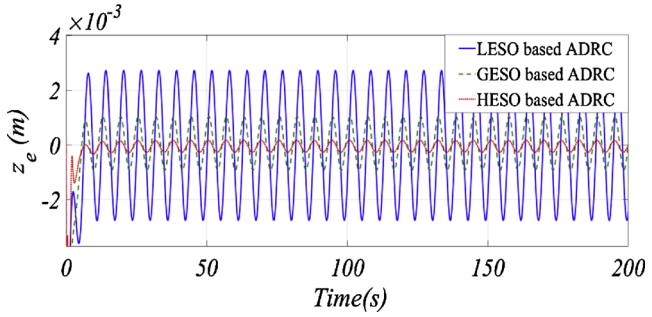

Fig. 8. Tracking errors comparison of HESO, GESO and traditional LESO in heading. tracking.

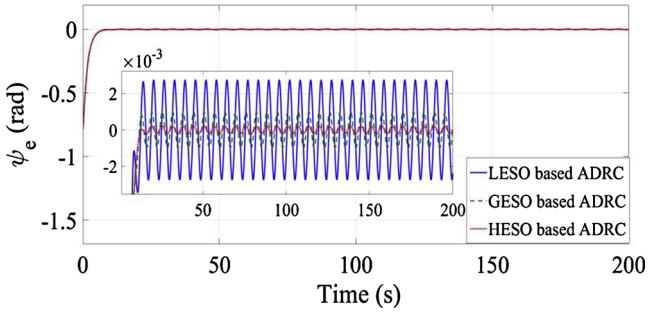

Fig. 9. Tracking errors comparison of HESO, GESO and traditional LESO in yaw tracking.

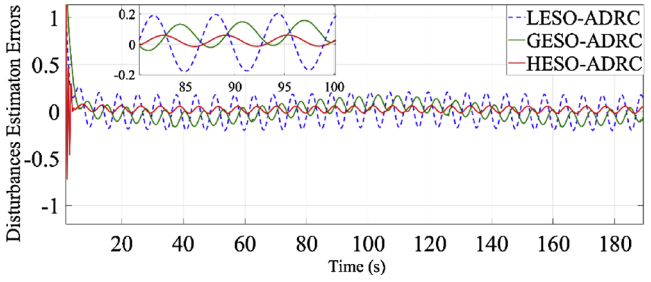

Fig. 10. Estimation errors comparison of HESO, GESO, and traditional LESO in surge tracking.

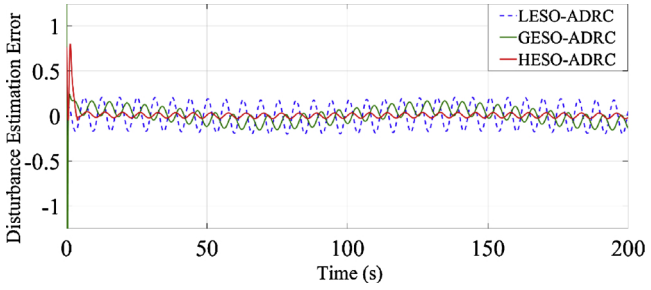

Fig. 11. Estimation errors comparison of HESO, GESO, and traditional LESO in sway tracking.

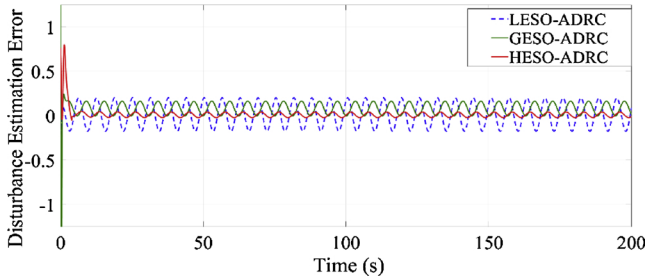

Fig. 12. Estimation errors comparison of HESO, GESO, and traditional LESO in heading tracking.

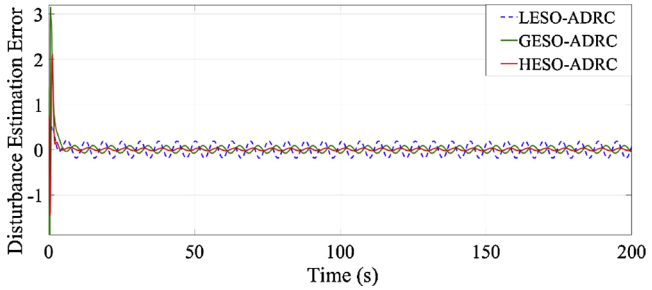

Fig. 13. Estimation errors comparison of HESO, GESO, and traditional LESO in yaw tracking.

$$\begin{cases} \beta_1 = 5\omega_0 \\ \beta_2 = 10\omega_0^2 \\ \beta_3 = 10\omega_0^3 \\ \beta_4 = 5\omega_0^4 \\ \beta_5 = \omega_0^5 \\ K_p = \omega_c^2 \\ K_d = 2\omega_c \end{cases} \tag{17}$$

where ω_o is the observer bandwidth and ω_c is the closed-loop bandwidth.

3.2. HESO

HESO is designed to estimate the periodic disturbances defined as:

$$d_i = A_i \sin(w_i t + \xi_i) + \sigma_i \tag{18}$$

with i is the considered DOF where the disturbances act, A_i, w_i, and ξ_i are disturbances amplitude, frequency, and phase, respectively, where σ_i is constant disturbance.

Motivated by the work done in [27], in order to enhance the periodic disturbances estimation quality, the 5th order HESO Eq. (20) which includes the disturbances dynamics in the classical ESO, is designed.

The space state of the disturbances dynamics is presented by Eq. (18)

$$\begin{cases} \dot{\lambda}_1 = \lambda_2 \\ \dot{\lambda}_2 = -\omega_i^2 \lambda_1 \\ d = \lambda_1 \end{cases} \tag{19}$$

By introducing Eq. (19) in the GESO (16), we obtain the HESO as

$$\begin{cases} \dot{z}_1 = z_2 - \beta_1 e_1 \\ \dot{z}_2 = z_3 - \beta_2 e_1 + b_x U_x \\ \dot{z}_3 = z_4 - \beta_3 e_1 \\ \dot{z}_4 = -\omega_i^2 z_3 + z_5 - \beta_4 e_1 \\ \dot{z}_5 = -\beta_5 e_1 \end{cases} \tag{20}$$

3.3. Control law

The control law for the 1 DOF illustrated in Fig. 2 is designed, then similar controllers are designed for the remaining DOFs.

$$U_x = \frac{U_0 - f_x}{b_1} \tag{21}$$

By replacing Eq. (21) in the dynamic equation of 1 DOF (surge equation), we obtain

$$\ddot{x} = f_x(\dot{x}, \dot{y}, \dot{\psi}, t, ds) + b_1\left(\frac{U_0 - f_x}{b_1}\right) \approx U_0 \tag{22}$$

The system can now be expressed as the following disturbance-free system

$$\begin{cases} \dot{x}_1 = x_2 \\ \dot{x}_2 = U_0 \\ y = x_1 \end{cases} \tag{23}$$

Where

$$U_0 = K_p(x_d - z_1) + K_d z_2 \tag{24}$$

By setting the controller gains, K_p and K_d, to ensure that the closed loop poles are located at – ω_c and to reach the Hurwitz stability.

3.4. Comments on stability

The GESO in Eq. (16) can be rewritten as

$$\dot{z} = \tilde{A}z + Bu \tag{25}$$

Where

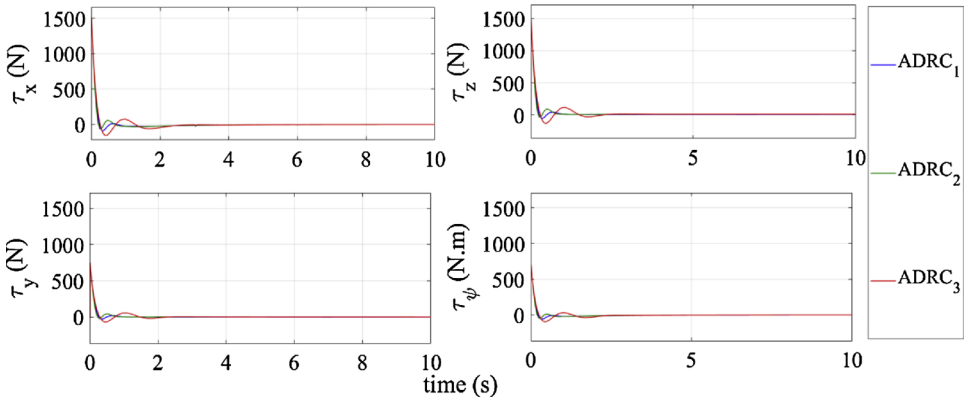

Fig. 14. Control laws.

$$\tilde{A} = \begin{bmatrix} -\beta_1 & 1 & 0 & 0 & 0 \\ -\beta_2 & 0 & 1 & 0 & 0 \\ -\beta_3 & 0 & 0 & 1 & 0 \\ -\beta_4 & 0 & 0 & 0 & 1 \\ -\beta_5 & 0 & 0 & 0 & 0 \end{bmatrix}, B = [0 \quad b_x \quad 0 \quad 0 \quad 0]$$

And $z = \hat{x}$. The estimation error is represented by $\tilde{x} = x - \hat{x} = x - z$.

Basing on the detailed stability analysis of the ESO and the entire ADRC based controllers made by Q. Zheng in [29] and stability analysis done in [30,31], the observer (Eq. (16)) parameters were chosen such that the characteristic polynomial is Hurwitz, thus, all the poles were placed at $-\omega_0$ as shown in Eq. (17). A brief stability analysis is presented below.

By assuming that $d_i^{(n)}$ is a Lipschitz continuous time signal, so $d_i^{(n)}$ is upper bounded with $\| d_i^{(n)} \| \leq D$.

Then, by choosing the Lyapunov function as $V(\tilde{x}_i) = -\tilde{x}_i^T P \tilde{x}_i$, where $\dot{V}(\tilde{x}_i) = \frac{\partial V(\tilde{x}_i)}{\partial t}$ is the derivative of the Lyapunov function, and i (i = x,y,z,ψ) represents the considered DOF (surge, sway, heading, or yaw).

$$\dot{V}(\tilde{x}_i) = \tilde{x}_i^T \tilde{A}^T P + P\tilde{A}\tilde{x}_i + 2\tilde{x}_i^T P\sigma_i \tag{26}$$

Since $\tilde{A}$ is Hurwitz, there exists a unique positive definite matrix P such that $\tilde{A}^T P + P\tilde{A} = -I$. So

$$\begin{aligned} \dot{V}(\tilde{x}_i) &= -\tilde{x}_i^T \tilde{x}_i + 2\tilde{x}_i^T P\sigma_i \leq -\| \tilde{x}_i \|^2 + 2 \| \tilde{x}_i \| \| P \| \| \sigma_i \| \\ &\leq -\| \tilde{x}_i \| (\| \tilde{x}_i \| - C) \end{aligned} \tag{27}$$

with $C = 2D\lambda_{\max}(P)$ and $\lambda_{\max}(P)$ is the maximum eigenvalue of P.

As conclusion, $\dot{V}(\tilde{x}_i) \leq 0$ is realized when $\| \tilde{x}_i \| \geq C$. Therefore, the input-to-state stability of the dynamic system describing the estimation error of the ESO in Eq. (16) has been proven.

In the same context, the control law in Eq. (21), kp and kd are the gain parameters of the controller (Eq. (24)) are chosen such as the closed loop poles are located at -ω_c in order to make the characteristic polynomial $s^2 + k_d s + k_p$ Hurwitz, which ensure the stability of the controller according to [29]. (Table 3)

4. Simulations and results

In order to verify the effectiveness of the designed HESO and GESO based ADRC control, they are applied to a 4 DOFs Fully-Actuated AUV. A set of simulations is performed in the Matlab Simulink. The AUV is set to track the desired path defined by Eq. (28) [28], The AUV's parameters are presented in Table 3.

$$\begin{cases} x_d = 10sin(0.01t) \\ y_d = 10cos(0.01t) \\ z_d = t \\ \psi_d = \frac{\pi}{4} \end{cases} \tag{28}$$

The external disturbances are the fast time-varying type specified as τ_w in Eq. (29)

$$\tau_\omega = \begin{bmatrix} d_x \\ d_y \\ d_z \\ d_\psi \end{bmatrix} = \begin{bmatrix} \sin(t) \\ 3\sin(t - \frac{\pi}{3}) + 2 \\ \sin(t) + 3 \\ 2\sin(t + \frac{\pi}{6}) \end{bmatrix} \tag{29}$$

The desired path and the actual three tracked paths in three dimension are shown in Fig. 3, the AUV can effectively follow the desired path, and track the desired positions and velocities with high accuracy as illustrated in Figs. 4 and 5. While Figs. 6–13 illustrates the positions tracking, and estimation errors in order to compare the performances of the LESO, GESO, and HESO based ADRCs (ADRC1, ADRC2, and ADRC3, respectively).

The tracking and estimation errors of the 3 different ESO based ADRCs are illustrated.

The trajectory tracking performances of the proposed controller with different ESOs are illustrated in Figs. 6–9. Compared to the traditional LESO, it can be clearly seen that the GESO-based ADRC offers better tracking performances in the 4 DOFs tracking, and the control accuracy was less affected by the external diturbances. However, more tracking accuracy improvements where noted for the HESO based ADRC which showed significant superiority in the tracking performances and the disturbances rejection.

In Figs. 10–13, it can be noted that the estimation errors decreased by employing the GESO compared to the LESO, where the HESO showed a higher estimation quality than both the GESO and LESO. This estimation enhancement has been ensured by embedding the dynamics of the disturbances in the full system state, as aresult the disturbances estimation quality has been improved, which has positively reflect on the tracking performances. The control laws are illustrated in Fig. 14.

By analyzing the obtained results on the background of some related works in [28–32], the following conclusions have been drawn:

- Compared to [28,32], in the tracking of 3D spiral path, our proposed approach decreased the tracking errors and convergence time.
- Compared to [33], the estimation and tracking ability of the conventional ADRC based control have been clearly improved.
- In [34,35]; observer-based robust controllers have been employed to cope with time-varying disturbances, and have offered very encouraging results. However, comparing to our proposed approach, the increasing of the observer's order and embedding the disturbances dynamics, have shown better disturbances estimation ability, and the tracking control performances of the path following control for AUVs.

5. Conclusion

In this paper, the path following problem of a fully-actuated AUV in the presence of fast-varying sinosoidal disturbances is investigated. In the proposed approach, we developed GESO and HESO based ADRC controllers in order to effectively attenuate the disturbance torque caused by waves and sea currents. It is shown that the GESO and HESO offer a significant enhancement in the tracking of fast-varying sinusoidal disturbances if the ESO bandwidth is set larger than the frequency of the disturbance, while the amplitude, phase, and bias are unknown. From the obtained results, we conclude that compared to the traditional 3rd order ESO, the GESO can ensure a better performance in estimating the sinusoidal disturbances, and the HESO offers better tracking and estimating performances than both the GESO and traditional LESO.

Conflicts of interest

Authors declare no conflicts of interest for the publication of this paper.

Author contributions

H.C.L has been the main author of the manuscript and did all the study design, data analysis, figures, and writing. Q.Z. (Qidan Zhu) is the work supervisor and he designed the paper with H.C.L and has revised the paper.

Funding

No funding has been received. This research was done during the Ph.D. study of H.C.L in Automation College of Harbin Engineering University.

Acknowledgments

We appreciate all editors and reviewers for the valuable suggestions and constructive comments. Thank you to everyone who contributed to this article

References

[1] T. Fossum, Intelligent autonomous underwater vehicles. Norwegian University of Science and Technology, Technol. Rep. (2016).
[2] J. Jackson, The US Naval Institute on Naval Innovation, Naval Institute Press, 2015.
[3] D.R. Blidberg, The development of autonomous underwater vehicles (AUV); a brief summary, IEEE ICRA (2001).
[4] P.G. Fernandes, P. Stevenson, A.S. Brierley, F. Armstrong, E.J. Simmonds, Autonomous underwater vehicles: future platforms for fisheries acoustics, ICES J. Mar. Sci. 60 (2003) 684–691.
[5] R.B. Wynn, V.A. Huvenne, T.P. Le Bas, B.J. Murton, D.P. Connelly, B.J. Bett, et al., Autonomous Underwater Vehicles (AUVs): their past, present and future contributions to the advancement of marine geoscience, Mar. Geol. 352 (2014) 451–468.
[6] S. Krupiński, G. Allibert, M.-D. Hua, T. Hamel, Pipeline tracking for fully-actuated autonomous underwater vehicle using visual servo control, American Control Conference (ACC) (2012) 6196–6202.
[7] X. Xiang, C. Yu, Q. Zhang, Robust fuzzy 3D path following for autonomous underwater vehicle subject to uncertainties, Comput. Oper. Res. 84 (2017) 165–177.
[8] N.R. Fischer, D. Hughes, P. Walters, E.M. Schwartz, W.E. Dixon, Nonlinear RISE-Based control of an autonomous underwater vehicle, IEEE Trans Robot. 30 (2014) 845–852.
[9] S. Liu, Y. Liu, N. Wang, Y. Fu, Adaptive fuzzy reaching law tracking control of uncertain fully-actuated underwater vehicles with system uncertainties and unknown disturbances, Control Conference (CCC), 2016 35th Chinese: IEEE, (2016), pp. 4476–4480.
[10] J. Gao, A.A. Proctor, Y. Shi, C. Bradley, Hierarchical model predictive image-based visual servoing of underwater vehicles with adaptive neural network dynamic control, IEEE Trans. Cybern. 46 (2016) 2323–2334.
[11] A.P. Aguiar, A.M. Pascoal, Dynamic positioning of an underactuated AUV in the presence of a constant unknown ocean current disturbance, Proc of the 15th IFAC World Congress, (2002).
[12] J. Han, From PID to active disturbance rejection control, IEEE Trans. Ind. Electron. 56 (2009) 900–906.
[13] Y. Wu, J. Sun, Y. Yu, Trajectory tracking control of a quadrotor UAV under external disturbances based on linear ADRC, Chinese Association of Automation (YAC), Youth Academic Annual Conference of: IEEE, (2016), pp. 13–18.
[14] H.C. Lamraoui, Z. Qidan, Speed tracking control of unicycle type mobile robot based on LADRC. Control science and systems engineering (ICCSSE), 2017 3rd IEEE International Conference on: IEEE, (2017), pp. 200–204.
[15] H.C. Lamraoui, Z. Qidan, A. Benrabah, Dynamic velocity tracking control of differential-drive mobile robot based on LADRC, Real-Time Computing and Robotics (RCAR), 2017 IEEE International Conference on: IEEE, (2017), pp. 633–638.
[16] F. Chen, H. Xiong, J. Fu, The Control and Simulation for the ADRC of USV. Chinese Automation Congress (CAC), IEEE, 2015, pp. 416–421.
[17] W. Changshun, Z. Huang, Y. Yu, USV Trajectory Tracking Control System Based on ADRC. Chinese Automation Congress (CAC), IEEE, 2017, pp. 7534–7538.
[18] Z. Yan, Y. Liu, J. Zhou, D. Wu, Path following control of an AUV under the current using the SVR-ADRC, J. Appl. Math. (2014).
[19] Y. Sun, Y. Zhang, G. Zhang, Y. Li, Path tracking control of underactuated AUVs based on ADRC, Proceedings of 2013 Chinese Intelligent Automation Conference, Springer, 2013, pp. 609–615.
[20] X. Yang, Y. Huang, Capabilities of extended state observer for estimating uncertainties, American Control Conference, 2009 ACC'09: IEEE, (2009), pp. 3700–3705.
[21] R. Madoński, P. Herman, Survey on methods of increasing the efficiency of extended state disturbance observers, ISA Trans. 56 (2015) 18–27.
[22] T.I. Fossen, Handbook of Marine Craft Hydrodynamics and Motion Control, John Wiley & Sons, 2011.
[23] N. Wang, C. Qian, J.-C. Sun, Y.-C. Liu, Adaptive robust finite-time trajectory tracking control of fully actuated marine surface vehicles, IEEE Trans. Control. Syst. Technol. 24 (2016) 1454–1462.
[24] S. Liu, Y. Liu, N. Wang, Nonlinear disturbance observer-based backstepping finite-time sliding mode tracking control of underwater vehicles with system uncertainties and external disturbances, Nonlinear Dyn. 88 (2017) 465–476.
[25] S. Liu, Y. Liu, N. Wang, Robust adaptive self-organizing neuro-fuzzy tracking control of UUV with system uncertainties and unknown dead-zone nonlinearity, Nonlinear Dyn. 89 (2017) 1397–1414.
[26] C. Yu, X. Xiang, L. Lapierre, Q. Zhang, Robust magnetic tracking of subsea cable by AUV in the presence of sensor noise and ocean currents, IEEE J. Ocean. Eng. 43 (2018) 311–322.
[27] D. Shi, Z. Wu, W. Chou, Harmonic extended state observer based anti-swing attitude control for quadrotor with slung load, Electronics 7 (2018) 83.
[28] B.K. Sahu, B.J.I. Subudhi, A. Jo, Computing. Adaptive Tracking Control Of An Autonomous Underwater Vehicle 11 (2014), pp. 299–307.
[29] Q. Zheng, On Active Disturbance Rejection Control: Stability Analysis and Applications in Disturbance Decoupling Control, Cleveland State University, 2009.
[30] D. Shi, Z. Wu, Chou WJIA, Generalized Extended State Observer Based High Precision Attitude Control of Quadrotor Vehicles Subject to Wind Disturbance, (2018).
[31] D. Shi, Z. Wu, W.J.E. Chou, Harmonic Extended State Observer Based Anti-Swing Attitude Control for Quadrotor with Slung Load 7 (2018), p. 83.
[32] J. Zhou, D. Ye, D. He, D. Xu, Three-dimensional trajectory tracking of an underactuated UUV by backstepping control and bio-inspired models, Control Conference (CCC), 2017 36th Chinese: IEEE, (2017), pp. 966–972.
[33] L. Habib Choukri, Q. Zhu, Path following control of fully actuated autonomous underwater vehicle based on LADRC, Polish Marit. Res. 25 (2018) 39–48.
[34] Z. Peng, J. Wang, Han Q-LJIToIE, Path-Following Control of Autonomous Underwater Vehicles Subject to Velocity and Input Constraints Via Neurodynamic Optimization, (2018).
[35] Z. Peng, J. Wang, J. Wang, JIToIE, Constrained Control of Autonomous Underwater Vehicles Based on Command Optimization and Disturbance Estimation 66 (2019), pp. 3627–3635.